THE UNIVERSITY OF
WARWICK

Original citation:
Daniels, D. Robert and Turner, Matthew S. . (2013) Islands of conformational stability for Filopodia. PLoS One, Vol.8 (No.3). Article no. e59010.
Permanent WRAP url:
http://wrap.warwick.ac.uk/53868

Copyright and reuse:
The Warwick Research Archive Portal (WRAP) makes the work of researchers of the University of Warwick available open access under the following conditions.

This article is made available under the Creative Commons Attribution-NonCommercial-NoDerivs 3.0 Unported (CC BY-NC-ND 3.0) license and may be reused according to the conditions of the license. For more details see: http://creativecommons.org/licenses/by-nc-nd/3.0/

A note on versions:
The version presented in WRAP is the published version, or, version of record, and may be cited as it appears here.

For more information, please contact the WRAP Team at: wrap@warwick.ac.uk

warwickpublicationswrap
highlight your research

http://go.warwick.ac.uk/lib-publications

OPEN ACCESS Freely available online

PLOS ONE

Islands of Conformational Stability for Filopodia

D. Robert Daniels[1]*, Matthew S. Turner[2]

1 Multidisciplinary Nanotechnology Centre, College of Engineering, Swansea University, Swansea, United Kingdom, **2** Department of Physics and Centre for Complexity Science, University of Warwick, Coventry, United Kingdom

Abstract

Filopodia are long, thin protrusions formed when bundles of fibers grow outwardly from a cell surface while remaining closed in a membrane tube. We study the subtle issue of the mechanical stability of such filopodia and how this depends on the deformation of the membrane that arises when the fiber bundle adopts a helical configuration. We calculate the ground state conformation of such filopodia, taking into account the steric interaction between the membrane and the enclosed semiflexible fiber bundle. For typical filopodia we find that a minimum number of fibers is required for filopodium stability. Our calculation elucidates how experimentally observed filopodia can obviate the classical Euler buckling condition and remain stable up to several tens of μm. We briefly discuss how experimental observation of the results obtained in this work for the helical-like deformations of enclosing membrane tubes in filopodia could possibly be observed in the acrosomal reactions of the sea cucumber *Thyone*, and the horseshoe crab *Limulus*. Any realistic future theories for filopodium stability are likely to rely on an accurate treatment of such steric effects, as analysed in this work.

Citation: Daniels DR, Turner MS (2013) Islands of Conformational Stability for Filopodia. PLoS ONE 8(3): e59010. doi:10.1371/journal.pone.0059010

Editor: Alexandre J. Kabla, University of Cambridge, United Kingdom

Received December 11, 2012; **Accepted** February 8, 2013; **Published** March 21, 2013

Copyright: © 2013 Daniels, Turner. This is an open-access article distributed under the terms of the Creative Commons Attribution License, which permits unrestricted use, distribution, and reproduction in any medium, provided the original author and source are credited.

Funding: These authors have no support or funding to report.

Competing Interests: The authors have declared that no competing interests exist.

* E-mail: d.r.daniels@swansea.ac.uk

Introduction

Filopodia are formed by the growth of bundles of biological fibers outwards from a biological cell surface that remain enclosed in a membrane tube. They are implicated in many processes vital to life, including sensing and motility [1] [2] [3]. There has therefore been much interest recently in the formation and growth of long, thin cellular protrusions due to the polymerization of bundles of fibers, including actin [4]. Such structures appear on cell membranes as familiar filopodia [1] [4], but can also appear on neural growth cones [5], sickled red blood cells [6] [7], the acrosomal reaction of the sea cucumber *Thyone* [8] [9], as well as on vesicles observed in vitro [10].

In this work, we investigate the stability of filopodia, which involves the subtle interplay between a fluid membrane tube, and an enclosed semiflexible fiber bundle. The simplest physical picture of filopodia is one in which the membrane tube produces a longitudinal force and a transverse force on the enclosed fiber bundle. The longitudinal membrane force acts to try and shorten the end-to-end distance of the fiber bundle, while the transverse force is required to maintain fiber bundle enclosure. The energetics required to investigate the stability of filopodia thus necessitates us to consider the elasticity of both the membrane tube as well as the fiber bundle, subject to the constraint that the polymer bundle must remain enclosed by the membrane tube. The energetic ground state conformations of filopodia thus necessitate a careful theoretical treatment of both elastic and steric considerations. For example, one might ask if a filopodium ever buckles, or perhaps more intriguingly does the region of filopodium buckling exist in some small corner of a complicated energetic phase diagram, well outside the range of physiologically relevant parameters?

A naive Euler buckling type estimate for the stability of filopodia [11] [12] suggests a limiting length of $1-2\mu m$. Additionally, the presence of cross-linking in the fiber bundle, and hence increased stiffness, further suggest a limiting length of $10-20\mu m$ for stable filopodia [11] [12]. However, filopodia many tens of μm have been observed experimentally [8] [13].

In [11], a helical ansatz was employed for the conformation of the polymer bundle. However, for analytical calculational purposes this was assumed to reside inside an enclosing membrane tube *that remained perfectly cylindrical*, despite simulation snapshot evidence to the contrary [11]. Energetically stable ground state configurations were calculated for filopodia within the range of physiologically relevant parameters. However, due to the presence of very soft modes [14] for membrane tube deformations, it is unrealistic to analytically assume that the enclosing membrane tube will remain perfectly cylindrical. It would cost the membrane tube very little energy to deform in order to accommodate the enclosed helical fiber bundle (see Fig. 1). In order to calculate analytically the ground state configurations of realistic filopodia, and their corresponding energetic stability, we find that it is necessary to explicitly compute the conformation of the enclosing membrane tube. This is achieved by minimising a rigorously derived energy functional (defined below) that includes the elastic response of both the membrane and the fiber bundle while respecting the constraint that the helical polymer bundle must remain enclosed by the membrane tube.

Results

Typical experimental parameter values for biological membranes range from [2] [15] $\kappa \approx 20-80 k_B T$, $\sigma \approx 0.0013-0.025 k_B T/\mathrm{nm}^2$. In order to compare the results of this work with that of [11], we take $\kappa = 40 k_B T$ and

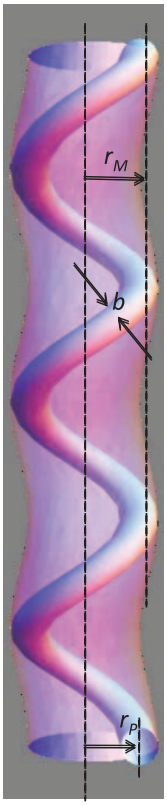

Figure 1. Sketch of a helically deformed membrane enclosing a helical fiber bundle. The membrane radius is given by r_M, the helical polymer radius is given by r_P, and b is the radial size of the enclosed polymer filament bundle.
doi:10.1371/journal.pone.0059010.g001

$\sigma = 0.0025 k_B T/\mathrm{nm}^2$ throughout in what follows. These values gives rise to a typical membrane tube radius of $r_0 \approx 89nm$. In order to estimate the radial size b of a filament bundle, we consider a cross-section of N fibers each with a typical size δ, which we assume forms a hexagonally close packed structure [9]. A suitable continuum approximation for the bundle radius b as a function of the number of fibers N is then : $b = \sqrt{1 + \frac{4(N-1)}{3}}\delta$, which approximates to $b(N) \simeq 2\sqrt{\frac{N}{3}}\delta$, for $N \gg 1$. If we take $\delta = 3nm$ (for actin filaments), and $N \sim 10 - 300$, then typical biological fiber bundles possess radii $b \sim 10 - 60nm$. Thus we can see that the finite radius filament bundle considerations contained in this work become important for physiological filopodia.

The ground-state configuration of a filopodium is determined by finding the minimum of the total energy per unit length $\frac{E_{tot}}{L}$ of Eq. (12) as given below. The relevant two parameters we need to minimise over are the z extension factor γ, and the helical radius of the enclosed fiber bundle r_P, while keeping the number of fibers N fixed.

Shown in Fig. 2 is the contour plot of the total energy per unit contour length $\frac{E_{tot}}{L}$ from Eq.(12). for a single fiber $N = 1$. The energy is plotted as a function of the enclosed filament helical radius r_P, and the z extension factor γ. It can be seen from Fig. 2 that, for the κ and σ values used, a single fiber does not give rise to a local energy minimum, and is therefore unstable. We find that the minimum number of fibers required for filopodium stability is given by $N = 4$, as shown in Fig. 3, which gives rise to a local energy minimum at: $r_P = 122nm$ and $\gamma = 0.77$, corresponding to one helical winding per $2\mu m$ of contour length. From Fig. 4 we can see that for $N = 20$ we have a local energy minimum at: $r_P = 99nm$ and $\gamma = 0.98$, corresponding to one helical winding per $4\mu m$ of contour length. Moreover, form Fig. 5 we can see that as the number of fibers N in a bundle increases, our filopodium remains stable, with the γ extension factor rapidly approaching the maximum allowed value of 1. Furthermore, as N increases, we can see from Fig. 6 that r_P decreases, tending towards the limiting value of $r_0 - b$, as the number of fibers becomes large. Additionally, we can see from Fig. 7 that the amount of helical winding required for stability reduces concomitantly also, as the number of fibers in a bundle N increases.

Discussion

We have calculated theoretically the ground state configurations of filopodia, and found 'islands of stability' for typical filopodia within physiologically relevant parameters. Our calculation elucidates how experimentally observed filopodia can obviate the classical Euler buckling condition and remain stable up to several tens of μm [1] [8] [13]. We find, as in [11] that the enclosing membrane tube tends to stabilise filopodia, rather than de-stabilise as a naive Euler buckling estimate might suggest.

The work presented here differs from that presented in [11] in the following, important ways. Firstly, we correctly incorporate the effects of a finite fiber bundle radial size b, in this work, which was absent in [11]. Secondly, the total energy $\frac{E_{tot}}{L}$ given by Eq.(12) of this work is calculated rigorously and analytically, taking into proper account the steric constraint of membrane tube enclosure of our semiflexible fiber bundle. The presence of soft modes for membrane tube deformations, implies that the membrane tube typically deforms in order to accommodate the enclosed helical fiber bundle, and does not remain perfectly straight, as analytically assumed in [11]. Thirdly, as we have found, there exists a delicate interplay between a fluid membrane tube and an enclosed semiflexible fiber bundle in filopodia. It is therefore imperative that the most accurate and correct total energy function for filopodia be calculated, as achieved in this work. Only then does it become possible to realistically describe the rather subtle issue of whether a given filopodium exists in a stable or a collapsed state. For example, we find in this work that the minimum number of fibers required for stability is given by $N = 4$, whereas in [11] all fibers with $N < 6$ are deemed unstable.

Experimental observation of the results obtained in this work for the helical-like deformations of enclosing membrane tubes in filopodia would presumably be difficult. However, such helical membrane conformations are qualitatively supported by the snapshot pictures of simulation work carried out in [11], and could possibly be observed in the acrosomal reactions of the sea cucumber *Thyone* [8], and the horseshoe crab *Limulus* [16].

We adopt a ground state approximation in which thermal fluctuations are assumed to be small. Since the amplitude of these fluctuations is small at the high tensions of interest to us here, perhaps a few nm or less [17], this is a reasonable approximation.

Analogous steric constraints to those considered here are likely to be of relevance in other similar and important biological contexts, such as the packaging of semiflexible DNA in viral capsids, for example [18] [19] [20]. The interesting issue of mechanical stability in biological cellular tubes *without* an enclosed stiff polymer has also recently been considered in [21].

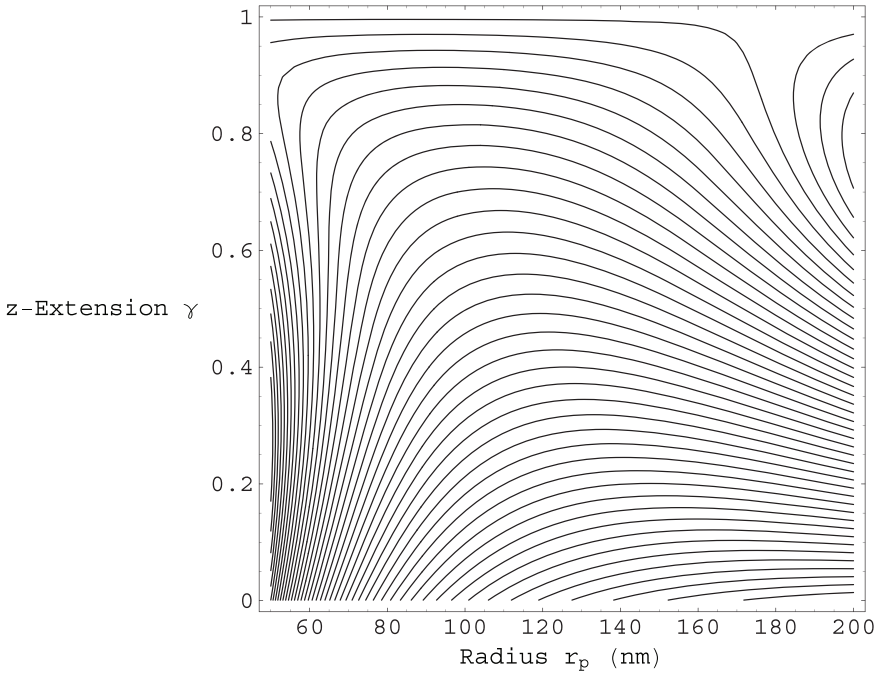

Figure 2. Contour plot of the total energy per unit contour length $\frac{E_{tot}}{L}$ from Eq.(12). The energy is plotted as a function of the enclosed filament helical radius r_P, and the z extension factor γ. The membrane bending modulus is $\kappa = 40 k_B T$ and the surface tension is $\sigma = 0.0025 k_B T/\mathrm{nm}^2$. The same values of κ and σ are used in all subsequent figures. The number of filaments in this case is given by $N = 1$. These parameters do not give rise to a local energy minimum. The contours near the top of the plot have values around $\sim 11pN$, those contours near the middle $\sim 7pN$, and the nearest to bottom contours on the plot $\sim 2pN$, (at room temperature).
doi:10.1371/journal.pone.0059010.g002

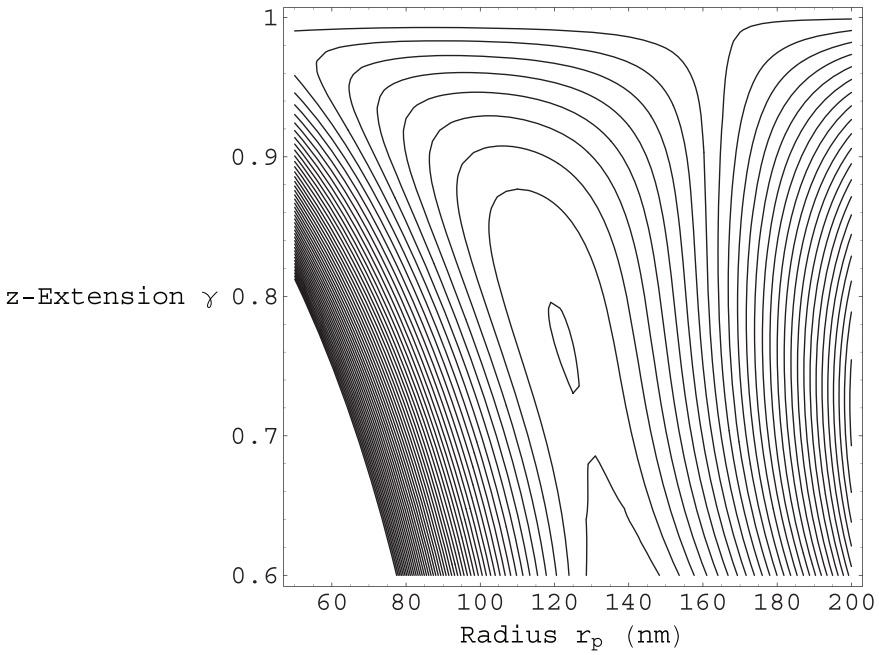

Figure 3. Contour plot of the total energy per unit contour length $\frac{E_{tot}}{L}$ from Eq.(12). The energy is plotted as a function of the enclosed filament helical radius r_P, and the z extension factor γ. The number of filaments in this case is given by $N = 4$. These parameters give rise to a local energy minimum at: $r_P = 122nm$ and $\gamma = 0.77$, corresponding to one helical winding per $2\mu m$ of contour length. Both the contours near the top and bottom of the plot have values around $\sim 12pN$, while the closed contour near the middle has a value of $\sim 10pN$.
doi:10.1371/journal.pone.0059010.g003

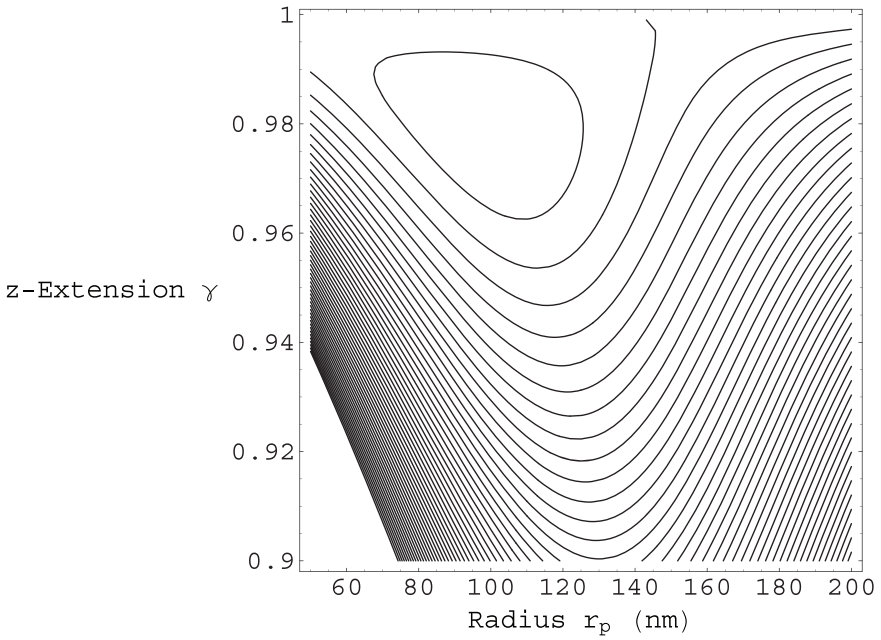

Figure 4. Contour plot of the total energy per unit contour length $\frac{E_{tot}}{L}$ from Eq.(12). The energy is plotted as a function of the enclosed filament helical radius r_P, and the z extension factor γ. The number of filaments in this case is given by $N=20$. These parameters give rise to a local energy minimum at: $r_P=99nm$ and $\gamma=0.98$, corresponding to one helical winding per $4\mu m$ of contour length. The closed contour near the top of the plot has a value of $\sim 11pN$, while the contours close to the bottom of the plot have values $\sim 13pN$.
doi:10.1371/journal.pone.0059010.g004

Models

Polymer Energy

In order to describe the filament bundle, inside filopodia, we study the semi-flexible polymer Hamiltonian H_p (where we chose energy units such that $k_{\mathrm{B}}T=1$ throughout):

$$H_P=\frac{l_p}{2}\int_0^L ds(\frac{\partial \mathrm{t}_3(s)}{\partial s})^2 \qquad (1)$$

with $t_3=\frac{\partial R_P(s)}{\partial s}$. L is the contour length of the fiber bundle, and we take the persistence length for un-crosslinked bundles of N fibers to be $l_p=\kappa_p N$ [12], where κ_p is the bending modulus of a single fiber ($\kappa_p\sim 15\mu m$ for actin [2]).

Any realistic deformation of the polymer must be able to pack a given contour length L within a given radius and extension along the z axis, as prescribed by the enclosing membrane tube. We therefore assume the most plausible conformation for the polymer as being that of a helix, as also outlined in [11].

$$\mathrm{R}_P(z)=r_P(\cos(\Omega z)\,\hat{\mathrm{i}}+\sin(\Omega \mathrm{z})\,\hat{\mathrm{j}})+\mathrm{z}\,\hat{\mathrm{k}} \qquad (2)$$

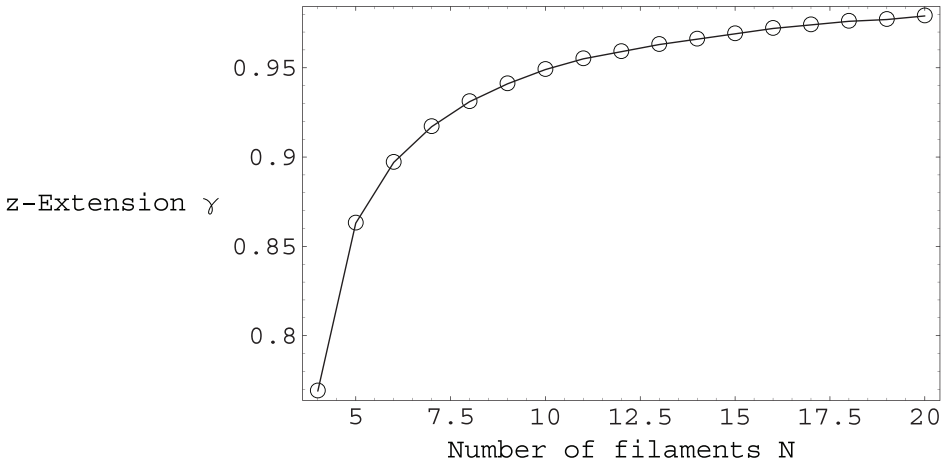

Figure 5. Plot of the extension factor γ along the z axis versus the number of filaments N. The γ values plotted correspond to the energetic minima of the total energy per unit contour length $\frac{E_{tot}}{L}$ from Eq.(12), for a given number of filaments N.
doi:10.1371/journal.pone.0059010.g005

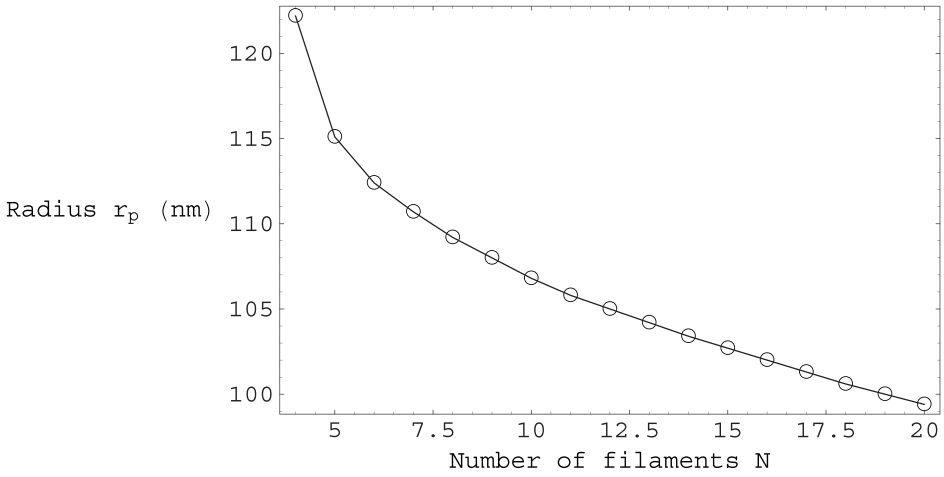

Figure 6. Plot of the polymer helical radius r_P versus the number of filaments N. The r_P values plotted correspond to the energetic minima of the total energy per unit contour length $\frac{E_{tot}}{L}$ from Eq.(12), for a given number of filaments N. For comparison, note that $r_0 \approx 89nm$.
doi:10.1371/journal.pone.0059010.g006

We have chosen to parameterise the polymer in terms of the z coordinate, as opposed to the arc-length s, in order to simplify consideration of the required steric constraint between the polymer and the membrane as outlined below. Inextensibility for the polymer is maintained by requiring that:

$$\gamma = \frac{dz}{ds} = \frac{1}{|\partial_z \mathrm{R}_P|} = \frac{1}{\sqrt{1+\Omega^2 r_P^2}} \tag{3}$$

In this way we can easily translate between the arc-length s, and z extension representations, by defining: $\frac{L_z}{L} = \gamma$ and $\omega = \gamma\Omega$, such that: $\gamma^2 + \omega^2 r_P^2 = 1$.

The polymer part H_P is thus straightforwardly calculated to be:

$$H_P = L\frac{l_p}{2}\frac{(1-\gamma^2)^2}{r_P^2} \tag{4}$$

Membrane Energy

In order to describe deformations of our membrane tube, we use:

$$H_M = \int \left[\sigma + \frac{\kappa}{2}c^2\right]\sqrt{g}ds\phi dz \tag{5}$$

where H_M is the usual Hamiltonian for membrane elasticity [22] [23], containing both surface tension (σ) and rigidity (κ) controlled terms.

We parameterise our membrane given by $R_M(z,\phi)$ in the usual way as:

$$\mathrm{R}_M(z,\phi) = r_M(z,\phi)(\cos(\phi)\,\hat{\mathrm{i}} + \sin(\phi)\,\hat{\mathrm{j}}) + z\,\hat{\mathrm{k}} \tag{6}$$

The membrane contribution H_M is calculated as follows. We proceed by writing perturbatively: $r_M(z,\phi) = r_0 + \delta r_M(z,\phi)$, which involves the radial length scale $r_0 = \sqrt{\frac{\kappa}{2\sigma}}$. In this way we obtain:

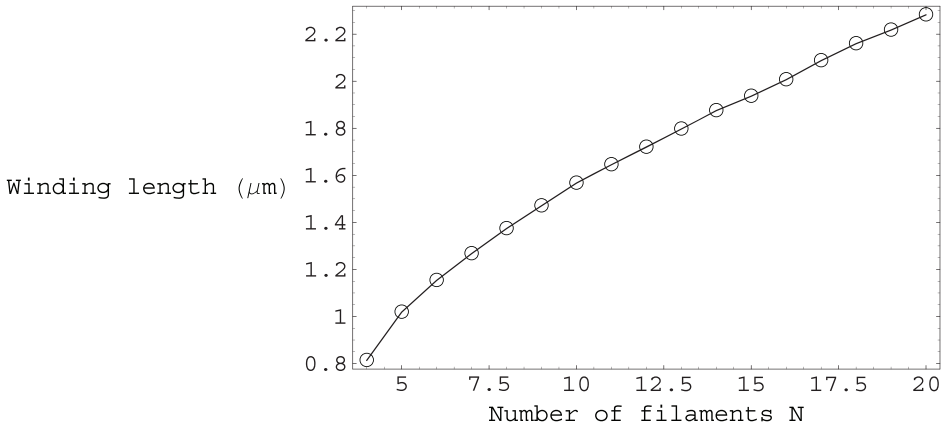

Figure 7. Plot of the polymer helical winding length versus the number of filaments N. The winding length values plotted correspond to the polymer contour length required for one complete helical turn in order to maintain stability of the filopodium.
doi:10.1371/journal.pone.0059010.g007

$$H_M = L_z \frac{2\pi\kappa}{r_0} + \frac{\kappa}{2r_0^3}\int d\phi dz\, \delta r_M(z,\phi) K_M\, \delta r_M(z,\phi) \qquad (7)$$

where the kernel K_M is given by: $K_M = (1+2\partial_\phi^2 + (r_0^2\partial_z^2 + \partial_\phi^2)^2)$.

Steric Constraint

By inspection of Eqs. (2) and (6), we can see that the steric condition we need to apply to the membrane in order to guarantee polymer enclosure is given by:

$$r_M(z,\Omega z) = r_P + b \qquad (8)$$

where b is the radial size of the polymer filament bundle. By writing perturbatively: $r_M(z,\phi) = r_0 + \delta r_M(z,\phi)$, the steric constraint of Eq. (8) now implies: $\delta r_M(z,\Omega z) = r_P + b - r_0$. We enforce this steric constraint by introducing the following Hamiltonian H_C:

$$H_C = \int dz \lambda(z)(\delta r_M(z,\Omega z) - (r_P + b - r_0)) \qquad (9)$$

which includes a Lagrange multiplier $\lambda(z)$ that ensures membrane tube enclosure of the confined polymer helix. While the steric relationship is strictly an inequality, on physical grounds the ground state polymer configuration always tends to contact the membrane because the longer the polymer the smaller the compressive load it can support before it buckles, becoming helical. Thus a long polymer will always tend to adopt a helical configuration, stabilised by the inward-pointing membrane force, at the maximum radius allowed by the steric constraint.

Total Energy

In order to find the ground-state configuration of our filopodium, we need to find the conformation which minimises the total energy E_{tot} given by: $E_{tot} = H_P + H_M + H_C$. By varying $H_M + H_C$ w.r.t. $\delta r_M(z,\phi)$ and $\lambda(z)$, and by using the relevant Green functions, we obtain:

$$\delta r_M(z,\phi) = (r_P + b - r_0) \sum_m a_m \cos(m(\phi - \Omega z)) \Big/ \sum_m a_m \qquad (10)$$

along with $\lambda(z) = -\frac{2\pi\kappa}{r_0^3}(r_P + b - r_0) / \sum_m a_m$, and where the Fourier coefficients a_m are given by: $a_m = 1/(1-2m^2 + m^4(1+\Omega^2 r_0^2)^2)$. Note that an ansatz loosely similar to Eq. (10) was also used in [24] to minimise the energy for a stack of n cylindrical membranes, in order to describe the helical coiling behaviour of myelin tubes. Indeed, the filopodia described in this work, consisting of a fiber bundle of radius b enclosed by a membrane tube, can analogously be thought of as an '$n=2$' cylindrical membrane stack. In terms of the Fourier coefficients a_m, the membrane radius solution of Eq. (10) can additionally be seen to automatically satisfy the steric constraint: $\delta r_M(z,\Omega z) = r_P + b - r_0$.

Putting the result of Eq. (10) into H_M we get (valid to quadratic order in $r_P + b - r_0$):

$$H_M = L_z \frac{2\pi\kappa}{r_0}\left(1 + \frac{(r_P + b - r_0)^2}{2r_0^2 \sum_m a_m}\right) \qquad (11)$$

By inspection of the Fourier coefficients a_m, it can be seen that for small Ω winding the leading order contribution to H_M comes from the $m=1$ mode, and is proportional to $\tilde{\Omega}^2$. This leads to a relatively weak strength for the quadratic potential in $r_P + b - r_0$, and is due to the fact that the $m=1$, $\Omega \simeq 0$ mode is an extremely soft mode for membrane tubes as shown in [14]. Indeed, the $m=1$, $\Omega = 0$ mode corresponds precisely to a rigid translation of the entire tube, and cannot therefore make any contribution to the membrane energy H_M. It can also be shown that the modes that contribute to H_M to next to leading order are the a_0 mode corresponding to a uniform dilation of the membrane tube, and the a_2 mode, which corresponds to a small deformation of the cross-section of our tube from a circular shape to that of an ellipse.

Utilising the inextensibilty conditions outlined above, we can easily re-write H_M in terms of the contour length L, and the z extension factor γ. In particular we find for the winding rate $\Omega = \frac{1}{r_P}\sqrt{\frac{1}{\gamma^2} - 1} \approx \frac{1}{r_0 - b}\sqrt{\frac{1}{\gamma^2} - 1}$, to leading order. We thus arrive at our final expression for the total energy per unit length of a filopodium as (valid to quadratic order in $r_P + b - r_0$):

$$\frac{E_{tot}}{L} = \frac{l_p}{2}\frac{(1-\gamma^2)^2}{r_P^2} + \frac{2\pi\kappa\gamma}{r_0}\left(1 + \frac{(r_P + b - r_0)^2}{2r_0^2 \sum_m a_m}\right) \qquad (12)$$

where the Fourier coefficients a_m are now functions of γ. The ground-state configuration of our filopodium can now be determined by minimising the total energy per unit length $\frac{E_{tot}}{L}$ of Eq. (12), with respect to the two parameters γ (the z extension factor) and r_P (the helical radius of the enclosed fiber bundle).

Acknowledgments

We would like to thank the anonymous referees for their helpful comments.

Author Contributions

Analyzed the data: DRD MST. Contributed reagents/materials/analysis tools: DRD MST. Wrote the paper: DRD MST.

References

1. Alberts B, Johnson A, Lewis J, Raff M, Roberst K, et al. (2002) Molecular Biology of the Cell. New York: Garland.
2. Boal D (2001) Mechanics of the Cell. Cambridge: Cambridge University Press.
3. Bray D (1992) Cell Movements. New York: Garland.
4. Mattila PK, Lappalainen P (2008) Filopodia: molecular architecture and cellular functions. Nat Rev Mol Cell Biol 9: 446–454.
5. Mitchison T, Kirschner M (1988) Cytoskeletal dynamics and nerve growth. Neuron 1: 761–772.
6. Briehl RW (1995) Nucleation, fiber growth and melting, and domain formation and structure in sickle cell hemoglobin gels. J Mol Biol 245: 710–723.
7. Daniels DR, Turner MS (2004) The force generated by biological membranes on a polymer rod and its response: Statics and dynamics. J Chem Phys 121: 7401–7407.
8. Tilney LG, Inoue S (1982) Acrosomal reaction of thyone sperm. ii. the kinetics and possible mech-anism of acrosomal process elongation. J Cell Biol 93: 820–827.
9. Daniels DR (2010) Effect of capping protein on a growing filopodium. Biophys J 98: 1139–1148.
10. Fygenson DK, Marko JF, Libchaber A (1997) Mechanics of microtubule-based membrane extension. Phys Rev Lett 79: 4497–4500.
11. Pronk S, Geissler PL, Fletcher DA (2008) Limits of filopodium stability. Phys Rev Lett 100: 258102.

12. Mogilner A, Rubinstein B (2005) The physics of filopodial protrusion. Biophys J 89: 782–795.
13. Wood W, Martin P (2002) Structures in focus - filopodia. Int J Biochem Cell Biol 34: 726–730.
14. Fournier JB, Galatola P (2007) Critical fluctuations of tense fluid membrane tubules. Phys Rev Lett 98: 018103.
15. Derenyi I, Julicher F, Prost J (2002) Formation and interaction of membrane tubes. Phys Rev Lett 88: 238101.
16. DeRosier DJ, Tilney L, Flicker P (1980) A change in the twist of the actin containing filaments occurs during the extension of the acrosomal process in limulus sperm. J Mol Biol 137: 375–389.
17. Daniels DR, Turner MS (2005) Spicules and the effect of rigid rods on enclosing membrane tubes. Phys Rev Lett 95: 238101.
18. Marenduzzo D, Micheletti C, Orlandini E (2010) Biopolymer organization upon confinement. J Phys - Cond Mat 22: 283102.
19. Morrison G, Thirumalai D (2009) Semiflexible chains in confined spaces. Phys Rev E 79: 011924.
20. Hu Y, Zandi R, Anavitarte A, Knobler CM, Gelbart WM (2008) Packaging of a polymer by a viral capsid: The interplay between polymer length and capsid size. Biophys J 94: 1428–1436.
21. Hannezo E, Prost J, Joanny JF (2012) Mechanical instabilities of biological tubes. Phys Rev Lett 109: 018101.
22. Safran SA (1994) Statistical Thermodynamics of Surfaces Interfaces and Membranes. Boston, MA: Addison Wesley Publishing.
23. Nelson D (1989) in Statistical Mechanics of Membranes and Surfaces. Singapore: World Scientific.
24. Santangelo CD, Pincus P (2002) Coiling instabilities of multilamellar tubes. Phys Rev E 66: 061501.